

AUTOMATED TECHNIQUE FOR CAROTID PLAQUE CHARACTERIZATION AND CLASSIFICATION USING RDWT IN ULTRASOUND IMAGES

¹Ms. Asha Kulkarni, Department of Electronics and Communication Engineering, JSS Polytechnic, Mysore, Karnataka, ashajssp@gmail.com

²Dr. Shashidhar SM, Principal, Proudhadivaraya Institute of Technology, Hosapete, Karnataka, shashi.com@gmail.com

Abstract

In this paper we proposed a Rational-Dilation Wavelet Transform (RDWT) technique to characterize plaques recorded from high-resolution ultrasound images and develop a Computer-Aided Diagnosis (CADx) model. The image acquisition and preprocessing, feature extraction and ensemble classifiers are automated for the classification of plaque. The transition bands are constructed by using the transition function. From the sub-bands mean, standard deviation, skewness, Renyi entropy and energy these statistical features are extracted. Salp Swarm Algorithm (SSA) is used for optimal features, the fundamental inspiration is the swarming behavior of slaps when navigating and foraging in oceans. K Nearest Neighbor (k-NN), Probabilistic Neural Network (PNN) and Support Vector Machine (SVM) classifiers are used in the Plaque Classification these techniques are compared in the classifier comparison. Experimental results show the accuracy, specificity and sensitivity of proposed method in terms of algorithm and classifiers. The percentage of accuracy in our method is 93%, the percentage of sensitivity in our method is 90% and the percentage of specificity in our ultrasound images. A texture feature analysis and classifiers for the automated carotid method is given as 94%.

Keywords: Rational-Dilation Wavelet Transform (RDWT), Computer-Aided Diagnosis (CAD), Salp Swarm Algorithm (SSA), classification.

1. Introduction

Cardiovascular disease (CVD) is the first leading cause of death in adults [1]. In [2], 80 million American adults of age 65 or older have one or more types of CVD. The survey says that 6 million deaths caused by CVD for most adult due to coronary heart disease and stroke. The significant factor for stroke is due to atherosclerosis [3]. Atherosclerosis is a condition in which the elasticity of the walls of the artery reduced thus narrowing the arteries [4, 5]. The atherosclerosis is distinguished by the buildup of lipids, cholesterol, smooth muscle, calcification in the inner walls of the artery [6]. The technique used to detect this kind of plaques is Carotid angiography [7]. But it is an invasive method; for the patients it is uncomfortable that would cause failure in kidney and the exposure to X rays [8]. In order to assess the severity of stenosis ultrasound, and echogenicity of plaque is taken into account. During the first phase of atherosclerosis plaque formation causes the blood vessel wall to expand without decreasing the diameter of lumen [9]. Particularly when dealing with artery stenosis plaque vulnerability depended on the plaque type which has serious consequence in future such as arterial occlusion or ischemic event in the brain. Endarterectomy reduces the risk of carotid stenosis hence risk of stroke is reduced [10]. Internal carotid stenosis based on plaque buildup is clinically established measure to quantitatively evaluate the risk for stroke.

In early, the MRI techniques [11] are used for carotid plaque imaging and diagnosis. The graph-search approach is used to detect the plaque and wall in intravascular ultrasound images. The noninvasive visualization of the carotid bifurcation is possible by high resolution ultrasound [12] has been used in study of arterial wall changes. Moreover, the texture features extracted from the ultrasound imaging of atherosclerosis carotid plaque may provide additional information to the physician for assessing risk in stroke and thereupon stroke treatment [13] thereby improving patient management [14, 15]. Further, through cardiac cycle the carotid plaque texture corresponds to plaque deformation and compresses the blood pressure. The affordable and cost effective is ultrasound imaging and for medical data acquisition, it is a good choice. It was shown that in the assessment of the atherosclerotic lesion increased the vulnerability of plaque [3]. In spite of significant diagnostic ultrasound advantages, low spatial resolution limits its usefulness [4]. Hence, using adequate image preprocessing techniques the ultrasonography image quality is improved and good features extraction may improve its accuracy of diagnostic.

The main objective of this paper is to develop a Computer-Aided Diagnosis (CADx) system using a texture feature analysis and classifiers for the automated carotid plaques characterization recorded from high-resolution ultrasound images. Using the standard model of classification carotid plaque can be better assessed and lead to better and accurate diagnosis. The features extracted from the ultrasound images help to characterize the feature parameters and help to develop systems which can intelligently classify plaques. Plaque is categorized into following types: (1) symptomatic due of ipsilateral hemispheric symptoms; (2) asymptomatic because they were not connected with ipsilateral hemispheric events. The primary aim is to assess a patient is at risk from stroke. Image acquisition and preprocessing, feature extraction using rational-dilation wavelet transform (RDWT), and ensemble classifiers for automated plaque classification are the methods used to help in the analysis of plaque. This paper is organized as follows; the brief review of related work is presented in section 2. Section 3 described our proposed system for automated plaque classification. Section 4 presents the result and discussion and finally, section 5 concludes the paper.

2. Related Work: A Brief Review

Various research works have already existed in literature which depended on the carotid plaque identification utilizing different methods and different perspectives. A portion of the works is reviewed on here.

Cheng et al. developed an algorithm that maps the counter plane of plaque from the images of ultrasound as discussed in there paper [16]. Based on lumen, the plaque surfaces were initialized and by semi-automatic algorithm the outer wall boundaries are generated. Then deformed, by a direct three dimensional sparse field level-set algorithm and enforced the longitudinal continuity of the segmented plaque surface. The presented 3D volume based algorithm requires for plaque segmentation, that is 40% lower than 2D slice-by-slice algorithm. Y. Hwang *et al.* [17] in their paper design classifier to identify coronary plaque regions using a hybrid ensemble from intravascular ultrasound (IVUS) images. extended binary discrete first level order the including level extracted cooccurrence local textural total IVUS matrix 102 gray hybrid statistics grey were matrix features a From features length run image pattern of intensity wavelet. Qian and Yang [18] developed a framework for identifying plaque segmentation. Four different classification algorithms were used to integrate features from ultrasound images. A probability map was generated based on the plaque segmentation.

The researcher in [19] developed a model of atherosclerotic plaque using image segmentation. In their work, the authors applied the snake algorithm to identify plaque in 44 subjects, 22 with and 22 without the plaque along the carotid axis. The resulting ICCs (inter class correlation coefficients) were significant for all three parameters namely mean echogenicity, perimeter and area. Using a different approach, U.Raghavendra *et al.* [20] have developed a CADx system for automated detection of coronary artery disease using echocardiography images taken from the four heart chamber. The methodology chosen for identify plaque is based on DD-DTDWT (double density- dual tree discrete wavelet transform). DD-DTDWT decomposes images into different sub-bands frequency and localizes the region of plaque formation. Furthermore, features dimension is reduced using MFA (marginal fisher analysis) and using feature ranking methods the optimal features are selected.

A reflection-mode all-optical laser ultrasound (LUS) imaging was presented by Jami L. Johnson et al [21]. Artery wall internal layers, vessel enlargement and calcification are observed with higher resolution and lower artifacts. To quantify the strain rate from the textural information of observed in ultrasound based carotid elastography help in discerning critical information about nature of plaque. Magnetic resonance imaging have also been used in studying plaque and its characteristics as presented by Chengwu Huang et al. [22]. Based on the gray-level co-occurrence matrix in plaque regions the four textural features like contrast, correlation, homogeneity and angular second moment of strain rate image was derived. The authors [23][24] have presented a noninvasive method for stoke risk assessment in patients with asymptomatic carotid atherosclerosis. By semi quantitative immune histo chemistry the plaque were assessed for vascular cell adhesion molecule, lectin like oxidized low-density lipoprotein receptor 1, p-selection and von willebrand factor.

2.1 Background of the Research Work

The review of the recent research work highlights the need for better frequency resolution in ultrasound images. However, there are many techniques have been implemented for carotid plaque identification by ultrasound images such as DD-DTDWT (double density- dual tree discrete wavelet transform), laser ultrasound (LUS), and learning-based integrated framework and so on.

Continuous wavelet transform (CWT) is utilized to inspect the signal of interest. Due to the operation of scaling and shifting, a continuous time two-dimensional representation of the signal of interest is achieved instead of the classical one dimensional frequency domain representations such as the Fourier transform. However, performing the CWT on a image leads to redundant information which results in high computational complexity thus making it not suitable for real time applications.

3. Materials and Methods

The schematic diagram of the proposed system is shown in figure.1. Initially, the carotid plaque ultrasound images are pre-processed and then subjected to feature extraction using RDWT technique. Subsequently, the significant features are extracted and the optimal feature is selected based on SSA. Then the selected features are fed to the SVM classifier for classification[32][33].

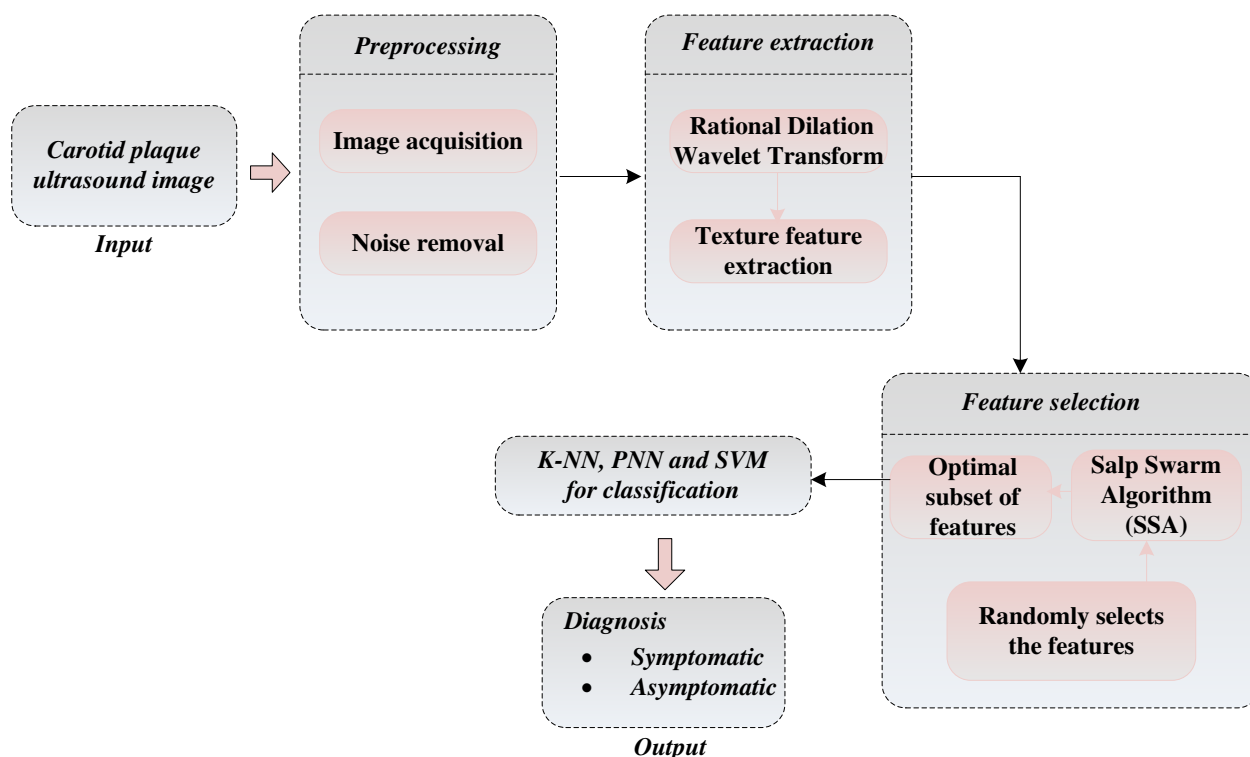


Fig.1. Schematic diagram of the proposed system

3.1 Image Acquisition and Preprocessing

3.2 Feature Extraction using RDWT

In signal processing applications, many over complete WTs like the double-density WT (DDWT) and the dual-tree complex WT (DTCWT) are utilized [20][22][23]. Only increasing the number of samples taken for few or all frequency bands in time WTs achieve over completeness and that stays the same sampling rate result in insufficient frequency resolution. However, in both time and frequency the sampling is increased and the RADWT can attain over-completeness which permits obtaining the optimum time-scale representation with controllable redundancy factors. Most of the discrete WTs utilize FIR-based ortho normal wavelet basis, the RADWT is based on a frequency-domain (FFT based) design which does not employ rational transfer functions and has flexibility design. Furthermore, the RADWT is a rational (non-dyadic dilations), fully discrete, near shift-invariant and invertible transform. The rational behavior of the RADWT provides a range of redundancy and Q-factors factors Feature extraction from the image texture characteristics is extracted using various texture analysis and image processing methods as presented in [23]. In the current work, RADWT are used to extract the features from ultrasound images, which is a multi resolution decomposition method. It decomposes an image into several sub-bands consisting of one approximation with detailed coefficients. A brief description of the methodology is given below. RADWT where RADWT and also like the two channel and a performed iterated are it of the through of in integers the and Q factor

on DWT built three wavelets Based satisfying structure filter bank positive coprime. In RADWT, the scaling parameter is A and the shifting parameter is B then set $\{A, B\}$ are permitted to take values from $\{Q^j / P^j, SPn/Q\}_{j,n \in \mathbb{Z}}$ which are controlled by P, Q and S [28].

In RADWT, the relation between the scaling ($\psi(t)$) and wavelet ($\phi(t)$) functions with the low pass filters and high pass filters are given as,

$$\psi(t) = (Q/P)^{1/2} \sum_{n \in \mathbb{Z}} H_0(n) \psi\left(\frac{Q}{P}t - n\right) \tag{1}$$

$$\phi(t) = (Q/P)^{1/2} \sum_{n \in \mathbb{Z}} G_0(n) \psi\left(\frac{Q}{P}t - n\right) \tag{2}$$

Where $H_0(n)$ and $G_0(n)$ represent the low-pass and high-pass filters, respectively.

The frequency responses of $H_0(n)(h_0(\omega))$ and $G_0(n)(g_0(\omega))$ are mathematically given as,

$$h_0(\omega) = \begin{cases} \sqrt{PQ} & \omega \in \left[0, \left(1 - \frac{1}{S}\right)\frac{\pi}{Q}\right], \\ \sqrt{PQ} \theta\left(\frac{\omega - A}{B}\right) & \omega \in \left[\left(1 - \frac{1}{S}\right)\frac{\pi}{Q}, \frac{\pi}{Q}\right], \\ 0 & \omega \in \left[\frac{\pi}{Q}, \pi\right], \end{cases} \tag{3}$$

$$g_0(\omega) = \begin{cases} 0 & \omega \in \left[0, \left(1 - \frac{1}{S}\right)\pi\right], \\ \sqrt{S} \theta_x\left(\frac{\omega - PA}{PB}\right) & \omega \in \left[\left(1 - \frac{1}{S}\right)\frac{\pi}{Q}, \frac{P}{Q}\pi\right], \\ \sqrt{S} & \omega \in \left[\frac{P}{Q}\pi, \pi\right], \end{cases} \tag{4}$$

Where, the scaling and shifting parameters are represented as

$$A = \left(1 - \frac{1}{S}\right)\frac{\pi}{P}, B = \frac{1}{Q} - \left(1 - \frac{1}{S}\right)\frac{1}{P} \tag{5}$$

The transition functions of $\theta(\omega)$ and $\theta_x(\omega)$ is defined as

$$\theta(\omega) = \frac{1}{2}(1 + \cos(\omega))\sqrt{2 - \cos(\omega)} \text{ for } \omega \in [0, \pi] \tag{6}$$

$$\theta_x(\omega) = \sqrt{1 - \theta^2(\omega)} \tag{7}$$

The transition function $\theta(\omega)$ bands construct used is of the transition $g_0(\omega)$ and $h_0(\omega)$ which originates from Daubechies' orthonormal wavelet filters with two vanishing moments. In the RADWT implementation, FFT based circular convolution for low-pass and high-pass filtering are used. The reconstruction of discrete signals of any length is provided by RADWT, when the length of the signal at each level is a multiple of the least common multiple of Q and S (denoted as $\text{lcm}(Q, S)$). Otherwise, the perfect reconstruction property is not suitable for circular convolution filtering operation. In the input signal zero-padding operation is applied in order to obtain the next multiple of $\text{lcm}(Q, S)$, while signal length does not satisfy this property. When the iterated filter-bank (number of levels go to infinity) is considered, the redundancy of the RADWT is found as follows.

$$\text{red}(P, Q, S) = \lim_{j \rightarrow \infty} \text{red}_j(P, Q, S) = \frac{1}{S} \frac{1}{1 - P/Q} \tag{8}$$

From these sub-bands the statistical features like mean, standard deviation, skewness, Renyi entropy and energy are extracted.

Calculation of statistical features

classifiers follows as or methods feed obtained standard matrix feature into and In vector entropy skewness to each energy of were mean Renyi deviation from values order extraction calculated;

The mean is the average intensity values of all image feature is calculated as,

$$\text{Mean} = \frac{1}{N} \sum_1^N X_i \tag{9}$$

Where, N is the number of input feature X_i . From the mean values, the intensity distribution is measured by standard deviation is expressed as:

$$SD = \left[\frac{1}{N-1} \sum_1^N (X_i - \text{Mean})^2 \right]^{1/2} \tag{10}$$

The unequal distribution of intensity values is measured using skewness.

$$\text{Skewness} = \frac{E(X_i - \text{Mean})^3}{SD^3} \tag{11}$$

The randomness of the distribution of intensity levels in feature X_i is measured by entropy. In the image the distribution is among greater intensity levels, if the value of entropy is high. This measurement is the inverse of energy and the entropy is calculated as:

$$\text{Entropy} = -\sum_i X_i^2 \log(X_i^2) \tag{12}$$

$$\text{Energy} = \frac{1}{N} \sum_1^N |X_i|^2 \tag{13}$$

After the calculation of these texture features the optimal features are selected using salp swarm algorithm (SSA) which is described in the following section.

3.3 Feature Selection

The high dimensional feature vectors heavily affect the classification performance. Hence the dimensionality of the feature vector is decreased by removing such insignificant and repetitive features by employing feature selection process.

3.3.1 SSA as a feature selector

The SSA is a novel algorithm proposed by S. Mirjalili [29] in 2017, the fundamental inspiration is the swarming behavior of slaps when navigating and foraging in oceans. Here, each feature subset of the carotid plaque can be seen as the salps position. Based on the maximum classification accuracy the best feature solution of the plaque is selected. At the beginning period of optimization process, the SSA investigates the search space and after that exploits it to keep up the harmony between the exploration and exploitation. The fitness function depends on two objectives namely; the number of selected features and the accuracy of the classifiers. In all iteration the best feature solutions are updated according to leader and followers. The steps for SSA are as follows,

Step 1: Initialization

of the first initialized steps expressed are to the positions competing of which SSA optimization other is similar the randomly step techniques salps,

$$P_i = rand * (U_i - L_i) + L_i \quad i = 1, 2, \dots, n \quad (14)$$

Where, P_i defines the initial position of the salps, U_i and L_i represents the upper and lower bounds respectively. $rand$ represents the random numbers uniformly generated in the range of [0, 1].

Step 2: Evaluation

In this step, for accuracy objective accuracy function calculated The calculating is the on each classification is based the evaluated as,

$$Accuracy(\%) = \frac{T_p + T_N}{T_p + F_N + F_P + T_N} \times 100 \quad (15)$$

Where, T_p and T_N represents the number of correct predictions with actual class as true and false respectively. F_N and F_P represents the number of incorrect predictions with the actual class as true and false respectively.

Step 3: Updating Leader Position

The source accompanying formula position based of on leader the respect salps is updated,

$$Pl_i = \begin{cases} F_j + R_1[(U_j - L_j)R_2 + L_j] & R_3 < 0.5 \\ F_j - R_1[(U_j - L_j)R_2 + L_j] & else \end{cases} \quad (16)$$

Where, Pl_i represents the position of the leader salp, F_j is the position of the food source in j th dimension and $R_1 - R_3$ are the uniform random numbers.

Step 4: Exploration and Exploitation

The most effective parameter in the SSA algorithm is the initial random number which makes the exploration and exploitation phases in the balanced state and it is expressed as,

$$R_1 = 2 \cdot \exp \left[- \left(\frac{4m}{I_{\max}} \right)^2 \right] \quad (17)$$

Where, m represents the current iteration and I_{\max} represents the maximum number of iterations.

Step 5: Updating Follower Position

The position of the followers salp are updated based on the Newton's law of motion which is revealed as,

$$Pf_j^i = \frac{t}{2} (at + 2v_o) \quad \forall i \geq 2 \quad (18)$$

Where, Pf_j^i represents the position of the i th follower salp in j th dimension, t is the time and v_o is the initial velocity which is assumed as zero. above optimization The process is time iteration between is 1 the represented formulated of iterations Then as the equation and as equals difference,

$$Pf_j^i = \frac{1}{2} (Pf_j^i + Pf_j^{i-1}) \quad \forall i \geq 2 \quad (19)$$

From the above conditions, the slap chains are simulated. The general technique of the SSA algorithm is appeared as the flowchart in fig. 2.

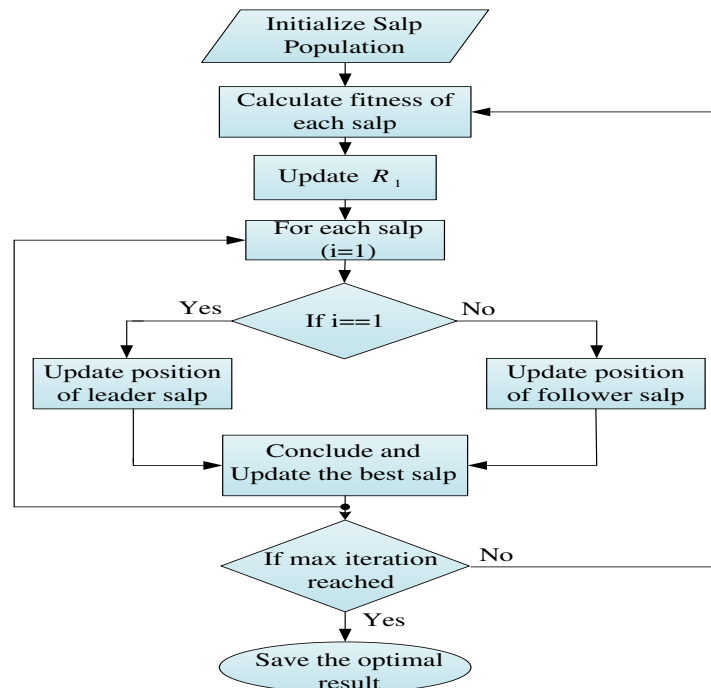


Fig.2. Flowchart of SSA

3.4 Plaque Classification

Each is classifiers classes hybrid a to a highly and work features as We model classification classifiers the in Vector SSA Probabilistic have k was Machine classification Network method region of are significant automated are model. In of asymptomatic brief ensemble used explained and selected form used kNN development. For automated Feature's detection PNN below symptomatic image descriptions process SVM subjected classifier Neural ensemble key an ranked a proposed ultrasound plaque of various of the inputs this. In system characterize Neighbor the used for Nearest Support[22][23].

From a set of training samples k-NN classifies the test data.[14] Around a target (i.e., unknown class) variable the training dataset nearest neighbors are located by computing the Euclidean distance between them. By a majority vote of its nearest neighbors the class of a test data is determined. A multi-layered feed forward neural network is PNN which can be used for classification[20]. To compute the weights, it uses supervised learning algorithm[15][16]. It is sensitive to outliers and required short training time.

A hyper plane-based nonparametric classifier is SVM[32][33]. Using input features-output ground truth class label pairs the SVM is trained and to test new input features it outputs used a decision function. For asymptomatic class assume that the class label $c = -1$ and for symptomatic class $c = 1$, the SVM algorithm maps the training set into a feature space and attempts to locate in that space a hyper plane and from the negative examples that separates the positive the feature a maximizes and functions separating first SVM the kernel which the non-separable determined features on classes into higher the are main hyper to During case that the testing Thus the which plane separating space an the of mapped is of to linearly the 30 determines maps algorithm class its the plane between is side then of unlabelled same based space sample data In present and a feature in hyper margin is input the sample space plotted the determine sample dimensional are the data using plane objective.

4. Experimental Results and Discussion

In this section, we perform several experiments that the accuracy, sensitivity and specificity of proposed RDWT methodology is evaluated. The algorithmic comparison, classification comparison, confusion matrix and the proposed performance window are performed in this section. All the experiments are implemented with MATLAB R2014a on a PC with 2.67 GHz Intel Xeon 12 CPU, RAM 16.00 G.

4.1 Dataset Description

The experiments in B- mode datasets [31] was related to the plaque classification project at Saint Mary’s Hospital, U.K. The database contains a total of 80 B-mode and blood flow longitudinal ultrasound images of the CCA. ATL HDI-3000 ultrasound scanner (Advanced Technology Lab- oratories, Seattle, USA) is used to acquire all the images and was recorded digitally on a magneto optical drive with a resolution of 768 x576 pixels with 256Gy levels. Digital images were resolution-normalized at 16.66 pixels/mm. When compared to the original B-mode ultrasound image the characteristics of normalized image change too much. Two ultrasound image scanners are used in the despeckle filters are ATL HDI-3000 and ATL HDI-5000.

4.2. Performance Analysis of evaluation metrics

The performance of proposed method is evaluated based on the following accuracy, sensitivity and specificity.

Accuracy: The measure of overall usefulness/ effectiveness of the classification technique are called accuracy. The equation for accuracy is

$$Accuracy (\%) = \frac{T_p + T_N}{T_p + F_N + F_P + T_N} \times 100 \tag{20}$$

Specificity: To recognize patterns of a negative class, it is used to measure the classifier ability. It is computed as follows.

$$sensitivity = \frac{t_p}{t_p + f_N} \tag{21}$$

Sensitivity: To recognize patterns of a positive class, it is calculated to measure the classifier ability. It is computed as follows

$$specificity = \frac{t_p}{t_p + f_N} \tag{22}$$

After the specificity it discuss about the confusion matrix and the proposed performance window. Confusion matrix is used to describe the performance of the classification model or classifier on the test of test data.

4.3 Comparison of Performance Metrics using Various Classifiers

The comparison between GA, PSO, WOA and proposed method for algorithmic comparison and the comparison between PNN, KNN, SVM and proposed method for classifier comparison is given as follows. It compares accuracy, specificity and sensitivity. Confusion matrix and the proposed performance window are also given in this section[32][33].

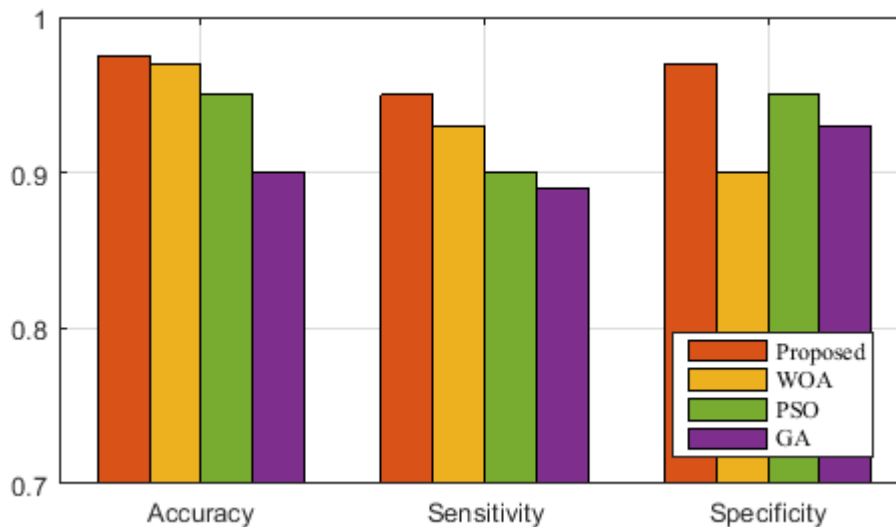


Fig 3: Algorithmic comparison Figure 3 shows the

comparison of algorithms which compares the accuracy, sensitivity and specificity of WOA, PSO, GA and proposed system[20]. From the figure it is clearly observed that, the performance of the proposed method is better than 0.08% of GA, 0.02% of PSO and 0.01% of WOA for accuracy. For sensitivity the performance of proposed method is better than 0.06% of GA, 0.05% of PSO, 0.02% of WOA. Similarly for specificity the performance of proposed method is better than 0.05% of GA, 0.02% of PSO and 0.08% of WOA.

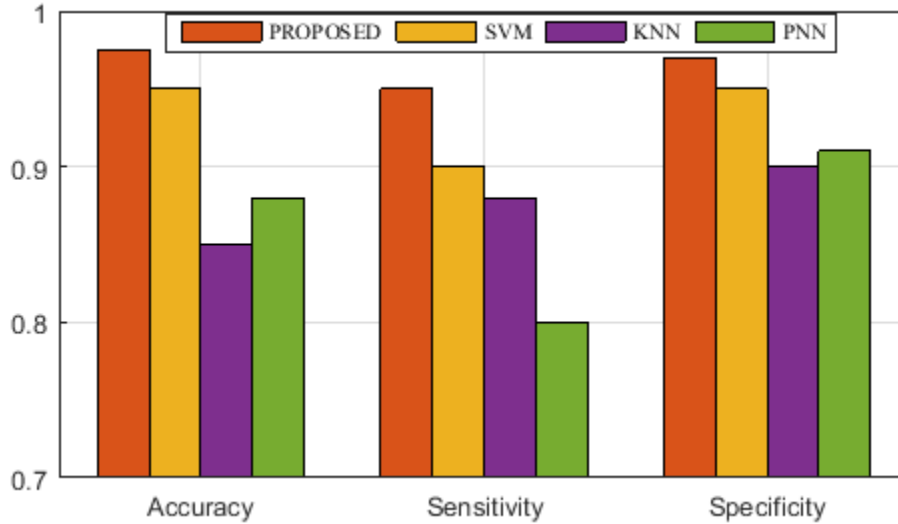


Fig 4: Classifier comparison

Figure 4 shows the classifier comparison it compares the accuracy, sensitivity and specificity of PNN, KNN and SVM with proposed method. From the figure it is clearly observed that, the performance of proposed method is better than 0.1% of PNN, 0.13% of KNN, 0.2% of SVM for accuracy. For sensitivity the proposed method is better than 0.16% of PNN, 0.07% of KNN and 0.06% of SVM. For specificity the proposed method is better than 0.06% of PNN, 0.07% of KNN and 0.02% of SVM.

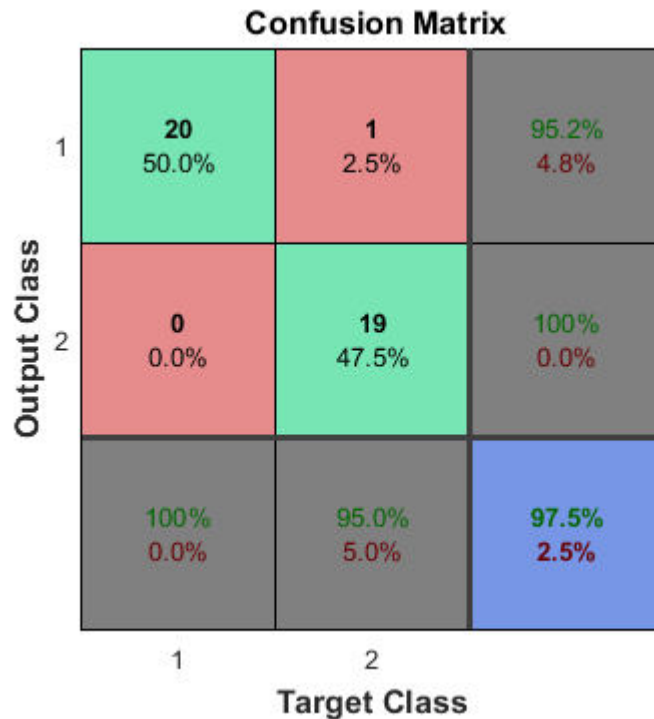


Fig 5: Confusion metrics window

A table model the confusion matrix true on set is known classification often or that to data test a of performance a is the used describe classifier are is values. The confusion matrix window is shown in figure 5. It shows both the target class and the output classes for the confusion matrix.

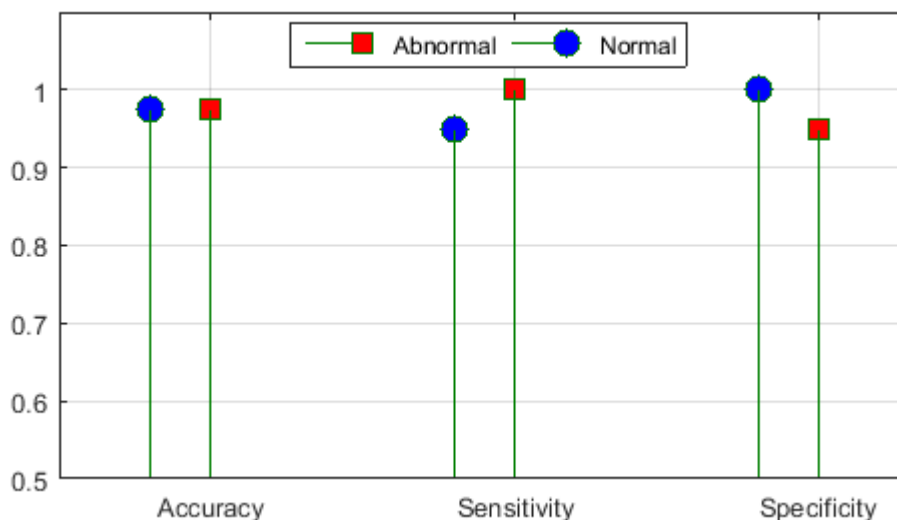


Fig 6: proposed performance window

Figure 6 shows the proposed performance window. It gives the normal and abnormal conditions of accuracy, sensitivity and specificity. At accuracy the normal and abnormal conditions are same. In sensitivity and specificity, the normal and abnormal conditions are differ. That is for sensitivity normal is low and abnormal is high, for specificity normal is high and abnormal is low.

5. Conclusion

The carotid plaque ultrasound images are pre-processed by using the RDWT. RDWT technique is used for feature extraction. In Plaque Classification consist of k Nearest Neighbor (k-NN), Probabilistic Neural Network (PNN) and Support Vector Machine (SVM) classifiers. The proposed systems have a high accuracy, sensitivity and specificity. The accuracy of proposed method is better of 0.08, 0.02, 0.01, 0.13 and 0.03. Sensitivity of the proposed method is better than 0.06, 0.05, 0.02, 0.18, 0.1 and 0.08. Specificity of the proposed method is better than 0.05, 0.02, 0.08, 0.06 and 0.07 when compare with other existing systems.

References

- [1] C. Qian and X. Yang, "An integrated method for atherosclerotic carotid plaque segmentation in ultrasound image", *Computer Methods and Programs in Biomedicine*, vol. 153, pp. 19-32, 2018.
- [2] W. Rosamond, K. Flegal, K. Furie, A. Go, K. Greenlund, N. Haase, S. Hailpern, M. Ho, V. Howard, B. Kissela, S. Kittner, D. Lloyd-Jones, M. McDermott, J. Meigs, C. Moy, G. Nichol, C. O'Donnell, V. Roger, P. Sorlie, J. Steinberger, T. Thom, M. Wilson and Y. Hong, "Heart Disease and Stroke Statistics--2008 Update: A Report From the American Heart Association Statistics Committee and Stroke Statistics Subcommittee", *Circulation*, vol. 117, no. 4, pp. e25-e146, 2007.
- [3] R. Hart, H. Diener, S. Coutts, J. Easton, C. Granger, M. O'Donnell, R. Sacco and S. Connolly, "Embolic strokes of undetermined source: the case for a new clinical construct", *The Lancet Neurology*, vol. 13, no. 4, pp. 429-438, 2014.
- [4] J. George, "Pathophysiology of Coronary Artery Disease", *Interventional Cardiology Imaging*, pp. 29-46, 2015.
- [5] R. Kamali, S. Kheirandish and K. Paktinat, "Investigation of Different Activities on the Hemodynamic Parameters of Left External Carotid Artery Using Fluid-Structure Interaction", *Iranian Journal of Science and Technology, Transactions of Mechanical Engineering*, 2018.

- [6] A. Sakamoto, S. Torii, H. Jinnouchi, A. Finn, R. Virmani and F. Kolodgie, "Pathologic intimal thickening: Are we any closer to understand early transitional plaques that lead to symptomatic disease?", *Atherosclerosis*, 2018.
- [7] A. Elder and M. Ng, "Iodide Mumps Complicating Coronary and Carotid Angiography", *Heart, Lung and Circulation*, vol. 26, no. 2, pp. e14-e15, 2017.
- [8] J. Amoedo, S. Ramió-Pujol, A. Bahí, L. Oliver, C. Puig-Amiel, P. Gilabert, A. Clos, M. Mañosa, F. Cañete, M. Serra-Pagès, J. Miquel-Cusachs, D. Busquets, M. Sabat, E. Domènech, J. Guardiola, J. Garcia-Gil and X. Aldeguer, "Su1828 - Raid-CD Monitor: A New Non-Invasive Method to Determine Endoscopic Activity in Patients with Inflammatory Bowel Diseases", *Gastroenterology*, vol. 154, no. 6, p. S-599, 2018.
- [9] U. Olgac, J. Knight, D. Poulidakos, S. Saur, H. Alkadhi, L. Desbiolles, P. Cattin and V. Kurtcuoglu, "Computed high concentrations of low-density lipoprotein correlate with plaque locations in human coronary arteries", *Journal of Biomechanics*, vol. 44, no. 13, pp. 2466-2471, 2011.
- [10] P. Rothwell, M. Eliasziw, S. Gutnikov, A. Fox, D. Taylor, M. Mayberg, C. Warlow and H. Barnett, "Analysis of pooled data from the randomised controlled trials of endarterectomy for symptomatic carotid stenosis", *The Lancet*, vol. 361, no. 9352, pp. 107-116, 2003.
- [11] A. Arias Lorza, A. van Engelen, J. Petersen, A. van der Lugt and M. de Bruijne, "Maximization of regional probabilities using Optimal Surface Graphs: Application to carotid artery segmentation in MRI", *Medical Physics*, vol. 45, no. 3, pp. 1159-1169, 2018.
- [12] G. Geroulakos, J. Domjan, A. Nicolaides, J. Stevens, N. Labropoulos, G. Ramaswami, G. Belcaro and A. Mansfield, "Ultrasonic carotid artery plaque structure and the risk of cerebral infarction on computed tomography", *Journal of Vascular Surgery*, vol. 20, no. 2, pp. 263-266, 1994.
- [13] A. Iannuzzi, T. Wilcosky, M. Mercuri, P. Rubba, F. Bryan and M. Bond, "Ultrasonographic Correlates of Carotid Atherosclerosis in Transient Ischemic Attack and Stroke", *Stroke*, vol. 26, no. 4, pp. 614-619, 1995.
- [14] H. Manoharan, et al., "Examining the effect of aquaculture using sensor-based technology with machine learning algorithm", *Aquaculture Research*, 51 (11) (2020), pp. 4748-4758.
- [15] S. Sundaramurthy, S. C and P. Kshirsagar, "Prediction and Classification of Rheumatoid Arthritis using Ensemble Machine Learning Approaches," *2020 International Conference on Decision Aid Sciences and Application (DASA)*, 2020, pp. 17-21, doi: 10.1109/DASA51403.2020.9317253.
- [16] P. R. Kshirsagar, H. Manoharan, F. Al-Turjman and K. Kumar, "DESIGN AND TESTING OF AUTOMATED SMOKE MONITORING SENSORS IN VEHICLES," in *IEEE Sensors Journal*, doi: 10.1109/JSEN.2020.3044604
- [17] Y. Hwang, J. Lee, G. Kim, E. Shin and S. Kim, "Characterization of coronary plaque regions in intravascular ultrasound images using a hybrid ensemble classifier", *Computer Methods and Programs in Biomedicine*, vol. 153, pp. 83-92, 2018.
- [18] C. Qian and X. Yang, "An integrated method for atherosclerotic carotid plaque segmentation in ultrasound image", *Computer Methods and Programs in Biomedicine*, vol. 153, pp. 19-32, 2018.
- [19] L. Bonanno, F. Sottile, R. Ciurleo, G. Di Lorenzo, D. Bruschetta, A. Bramanti, G. Ascenti, P. Bramanti and S. Marino, "Automatic Algorithm for Segmentation of Atherosclerotic Carotid Plaque", *Journal of Stroke and Cerebrovascular Diseases*, vol. 26, no. 2, pp. 411-416, 2017.
- [20] P. R. Kshirsagar and S. G. Akojwar, "Prediction of neurological disorders using optimized neural network," *2016 International Conference on Signal Processing, Communication, Power and Embedded System (SCOPES)*, 2016, pp. 1695-1699, doi: 10.1109/SCOPES.2016.7955731.

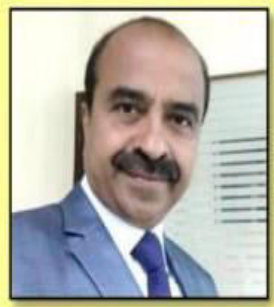
- [21]J. Johnson, M. Merrilees, J. Shragge and K. van Wijk, "All-optical extravascular laser-ultrasound and photoacoustic imaging of calcified atherosclerotic plaque in excised carotid artery", *Photoacoustics*, vol. 9, pp. 62-72, 2018.
- [22]Pravin Kshirsagar, Nagaraj Balakrishnan & Arpit Deepak Yadav "Modelling of optimised neural network for classification and prediction of benchmark datasets", *Computer Methods in Biomechanics and Biomedical Engineering: Imaging & Visualization*, 8:4, 426-435, DOI: 10.1080/21681163.2019.1711457,2020
- [23]Dr. Sudhir Akojwar, Pravin Kshirsagar, Vijetalaxmi Pai "Feature Extraction of EEG Signals using Wavelet and Principal Component analysis", *National Conference on Research Trends In Electronics, Computer Science & Information Technology and Doctoral Research Meet*, Feb 21st & 22nd ,2014.
- [24]Kshirsagar, P.R., Akojwar, S.G., Dhanoriya, R, " Classification of ECG-signals using artificial neural networks", In: *Proceedings of International Conference on Intelligent Technologies and Engineering Systems*, Lecture Notes in Electrical Engineering, vol. 345. Springer, Cham (2014).
- [25]U. Acharya, S. Sree, R. Ribeiro, G. Krishnamurthi, R. Marinho, J. Sanches and J. Suri, "Data mining framework for fatty liver disease classification in ultrasound: A hybrid feature extraction paradigm", *Medical Physics*, vol. 39, no. 71, pp. 4255-4264, 2012.
- [26]U. Acharya, M. Mookiah, S. Vinitha Sree, D. Afonso, J. Sanches, S. Shafique, A. Nicolaidis, L. Pedro, J. Fernandes e Fernandes and J. Suri, "Atherosclerotic plaque tissue characterization in 2D ultrasound longitudinal carotid scans for automated classification: a paradigm for stroke risk assessment", *Medical & Biological Engineering & Computing*, vol. 51, no. 5, pp. 513-523, 2013.
- [27]U. Acharya, S. Sree, M. Muthu Rama Krishnan, N. Krishnananda, S. Ranjan, P. Umesh and J. Suri, "Automated classification of patients with coronary artery disease using grayscale features from left ventricle echocardiographic images", *Computer Methods and Programs in Biomedicine*, vol. 112, no. 3, pp. 624-632, 2013.
- [28]I. Selesnick and İ. Bayram, "Oscillatory plus transient signal decomposition using overcomplete rational-dilation wavelet transforms", *Wavelets XIII*, 2009.
- [29]S. Mirjalili, A. Gandomi, S. Mirjalili, S. Saremi, H. Faris and S. Mirjalili, "Salp Swarm Algorithm: A bio-inspired optimizer for engineering design problems", *Advances in Engineering Software*, vol. 114, pp. 163-191, 2017.
- [30]V. Sánchez A, "Advanced support vector machines and kernel methods", *Neurocomputing*, vol. 55, no. 1-2, pp. 5-20, 2003.
- [31] C. Qian, X. Yang, "An integrated method for atherosclerotic carotid plaque segmentation in ultrasound image", *Computer methods and programs in biomedicine*, vol. 153, pp. 19-32, 2018.
- [32]S. Akojwar and P. Kshirsagar, "A Novel Probabilistic-PSO Based Learning Algorithm for Optimization of Neural Networks for Benchmark Problems", *Wseas Transactions on Electronics*, Vol. 7, pp. 79-84, 2016.
- [33]Sudhir G. Akojwar, Pravin R. Kshirsagar, " Performance Evolution of Optimization Techniques for Mathematical Benchmark Functions". *International Journal of Computers*, **1**, 231-236,2016.

Authors Profile



Asha kulkarni received BE degree in ECE from SLN college of Engineering, Raichur, affiliated to Gulbarga University, Gulbarga, Karnataka in 1990. MTech Degree in

VLSI&ES from SJCE , Mysore, Karnataka in 2008 . She is currently working toward the PhD degree at the Department of Electrical Engineering, VTU, Belagavi, Karnataka. Her research interest includes VLSI and Medical Electronics. Presently working as Head of Department of ECE at JSS Polytechnic, Mysore, Karnataka, since 1997



Dr. Shashidhar SM received BE degree in EEE from BDT Engineering College, Davangere affiliated to Mysore University, Karnataka in 1985. ME in Power Electronics from PDA College of Engineering, Gulbarga, Karnataka in 1989. PhD from SV University Tirupati in 2015. Presently working as Principal of Proudhadavaraya Institute of Technology , Hosapete, Karnataka.